# SIGNAL PROCESSING AND NOISE REDUCTION OF A FIBER BRAGG GRATING SEISMIC SENSOR SYSTEM

*J.-G. Liu, C. Schmidt-Hattenberger, and G. Borm*

GeoForschungsZentrum Potsdam (GFZ), Div. 5 "Geomechanics and Geotechnology"
Telegrafenberg, D-14473 Potsdam, Germany
Phone: +49-331-288-1550/1552, Fax: +49-331-288-1502, e-mail: jgliu@gfz-potsdam.de

**Abstract –** *Fiber optic Bragg gratings have found increasing applications to seismic strain measurement of underground structures and rock mass. The strain sensitivity of a Bragg grating measuring system, however, is limited by the noise caused by the instability of the laser wavelength and the rough measurement surroundings. Signal processing and noise reduction plays therefore an important role in the strain measurement using fiber Bragg gratings. In this paper discrete autocorrelation function and iterative smoothing are applied to the improvement of the signal to noise ratio and the detectability of seismic signals in underground rock mass. Results from laboratory and field experiments are given to show the noise reduction and detectability improvements.*

**Keywords -** Fiber Bragg grating, seismic monitoring, noise reduction, autocorrelation function, iterative numerical smoothing

## 1. INTRODUCTION

The measurement of rock deformations is increasingly interesting in underground structures and mines, since underground excavations and blasting works generally create changes in the stress regime of the surrounding strata [1]. Fiber optic Bragg grating seismic system plays a significant role in monitoring/recording the actual seismic responses of underground structures and rock mass.

Typical elements for supporting underground excavations in hard rock are reinforcing steel meshes and glassfiber reinforced polymer (GRP) rockbolts mounted in boreholes radically to the tunnel axis. An idea is to use the rockbolts simultaneously as sensor heads for monitoring dynamic deformations by embedding Bragg gratings into anchor rods [1]. A Fiber Bragg Grating (FBG) seismic sensor system has been developed for the detection of strain vibrations in underground rock mass excavations [3].

The sensitivity of this measuring system, however, is limited by the noise caused from the laser wavelength instability, disturbance, and the rough measurement surroundings in underground structures. To improve the signal to noise ratio of the measuring system, the sensor structure has to be optimized and the laser source should be further stabilized on one hand, and noise must be reduced by signal processing on the other hand [2].

In the following sections a background about the measuring principle of Bragg grating and wavelength optimization of the laser source is given. Signal processing and noise reduction methods are described, and results from laboratory and field experiments are discussed in detail.

## 2. BACKGROUND

The scheme of the fiber Bragg grating seismic sensor system is shown in Fig.1. The sensor-head consists of a glassfiber reinforced polymer (GRP) rockbolt in which the grating is glued by epoxy resin.

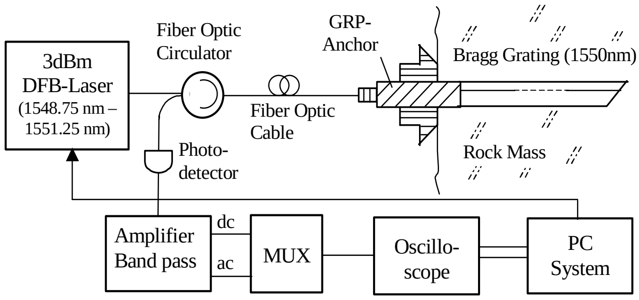


Fig. 1 Experimental setup for data acquisition of dynamic seismic strain signals in underground rock mass

A distributed feedback laser (DFB-Laser) with a wavelength range from 1548.75 nm to 1551.25nm sends an optic signal to the fiber Bragg grating through a fiber optic circulator. A part of the optic signal is reflected from the Bragg grating and back through the circulator to a photo-detector. This reflected signal is converted into an electrical signal. The signal is amplified, filtered and then sampled with an oscilloscope. The sampled signal is processed in a PC system.

The intensity of the reflected optic signal is a function of the Bragg grating period which relates to the applied strain on the Bragg grating. Therefore the dynamic strain can be derived from the intensity change measurement as function of the wavelength of the reflected optic signal [3].

In order to realize a maximal sensitivity of the strain measurement, the wavelength of the applied DFB-laser is optimized by dc photovoltage measurement. Fig. 2 shows the photovoltage from the pre-amplifier and sensitivity as function of the wavelength of the laser source. The maximum photovoltage is at the wavelength of 1549.95nm for the

ISBN 972-98115-4-7  

experimental fiber optic Bragg grating system. The first maximal sensitive point is located at the wavelength of $\lambda_{o1}$=1549.86nm, while the second maximal sensitive point is at $\lambda_{o2}$=1550.05nm.

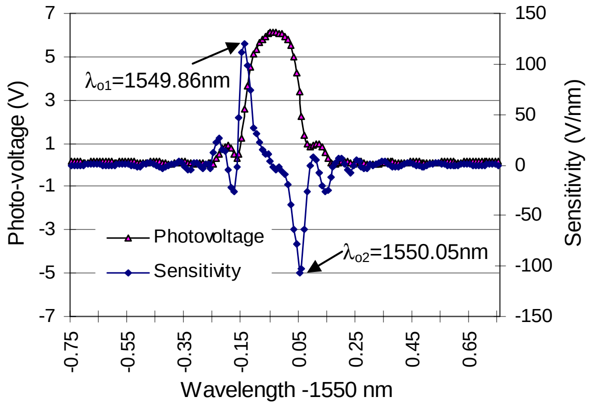


Fig.2 Effective value of dc photovoltage and sensitivity derived from the dc photo-voltage

To choose the better one from the two optimized wavelengths, the effective noise values at these two wavelengths are measured within a bandwidth of 100 Hz to 5 kHz. A measure is defined by

$$m = \frac{S}{rms} \tag{1}$$

as criteria, where $S$ and $rms$ denote the sensitivity and the effective noise value, respectively. The wavelength with a higher value of $m$ will be used for the measurement.

The strain sensitivity of this measuring system is limited by the noise caused by the instability of the laser wavelength, disturbance, and measurement conditions. Fig. 3 shows the *rms*-values of the original noise. The effective value of the noise reaches its maximum in the most sensitive wavelength range.

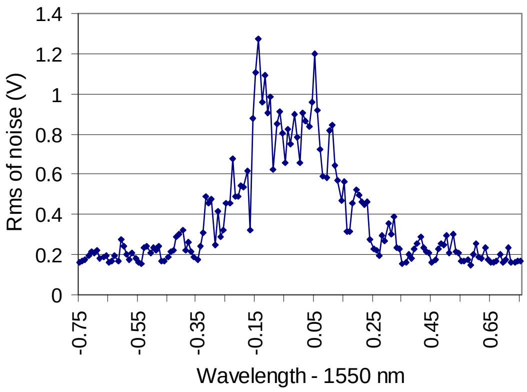


Fig.3 Effective values of ac photovoltage as function of wavelength

It is difficult to reduce the noise by a band pass filtering since the magnitude spectrum of the signal is superimposed by the noise spectra (Fig. 4). Seismic signals are usually in the low frequency range of 100 Hz to 5 kHz. In this case strain variations down to $10^{-9}$ can be detected. This corresponds with the results in first field experiments presented in [1].

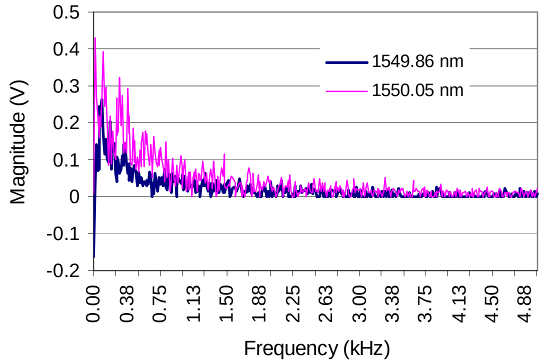


Fig. 4 Magnitude spectrum of noise at optimized wavelengths

## 3. SIGNAL PROCESSING

To reduce the noise, special methods like iterative numeric smoothing, autocorrelation functions, and discrete Fourier-Transformation are used for signal processing.

### 3.1 Iterative Numeric Smoothing

The numeric smoothing has the property of a low pass filter. In order to smooth the sampling value $x_k$ ($k$=0, 1, 2, …, $N$-1) at sampling point $t_k$ a polynomial of 3. order $P(t)$ is putted through 5 sampling points. The value of the polynomial at the position $t_k$ is defined as the smoothing value $y_k$. The output signal $y_k$ is written by [5]

$$y_k = \frac{1}{35}(-3x_{k-2} + 12x_{k-1} + 17x_k + 12x_{k+1} - 3x_{k+2}) \tag{2}$$

with $k$=2, 3, ..., $N$-3.

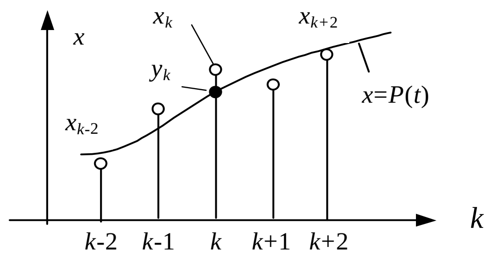


Fig. 5 Smoothing using a polynomial and 5 sampling points

For smoothing the first two ($k$=0,1) and last two ($k$=$N$-2, $N$-1) sampling values the following equations are used, i.e. [5]:

$$\begin{cases} y_0 = \frac{1}{70}(69x_0 + 4x_1 - 6x_2 + 4x_3 - x_4) \\ y_1 = \frac{1}{35}(2x_0 + 27x_1 + 12x_2 - 8x_3 + 2x_4) \\ y_{N-2} = \frac{1}{35}(2x_{N-5} - 8x_{N-4} + 12x_{N-3} + 27x_{N-2} + 2x_{N-1}) \\ y_{N-1} = \frac{1}{70}(-x_{N-5} + 4x_{N-4} - 6x_{N-3} + 4x_{N-2} + 69x_{N-1}) \end{cases} \tag{3}$$

For an iterative smoothing the output signal $y_k$ is assigned to the input signal $x_k$. Therefore a further smoothing can be carried out by (2) and (3) using the new input signal.

After one smoothing the noise reduction ratio, which is defined as the ratio of the noise effective value before processing to the noise effective value after the processing, is about $\sqrt{2}$ according to [6]. The reduction ratio increases to $\left(\sqrt{2}\right)^M$ if $M$ iterative smoothing is used.

### 3.2 Discrete Autocorrelation

Uncorrelated noise can considerably be reduced by a discrete autocorrelation function which separates the noise from the signal using the property of band-pass filter.

For a discrete input signal $x_k$ ($k$=0,1,2…, $N$-1), two time windows are used for calculating a discrete autocorrelation function. Each window contains $N_1$ sampling points. The first window is fixed at the beginning of the time axis, while the second window moves from the beginning to the end of the time axis with a delay time $t_n$ (Fig. 6).

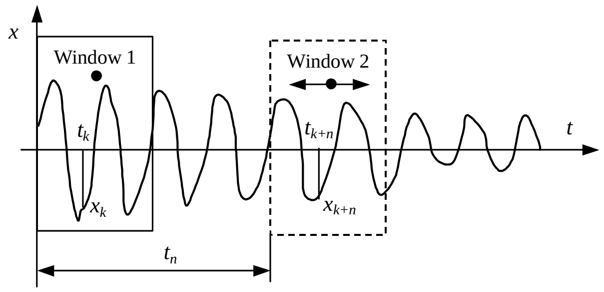


Fig. 6 Autocorrelation function using fixed and movable windows

The autocorrelation function is defined by

$$y_n = \lim_{N_1 \to \infty} \frac{1}{N_1} \sum_{k=0}^{N_1 - 1} x_k x_{k+n} \text{ , } (n=0,1,\ldots, N\text{-}N_1) \qquad (4)$$

The windows should contain $P$ signal periods, normally $1 \leq P \leq 10$. The noise reduction depends on the sampling number $N_1$ within the windows. The number $N_1$ should be high enough to reduce the noise effectively. The noise reduction ratio of the autocorrelation is about $0.5\sqrt{N_1}$ [6].

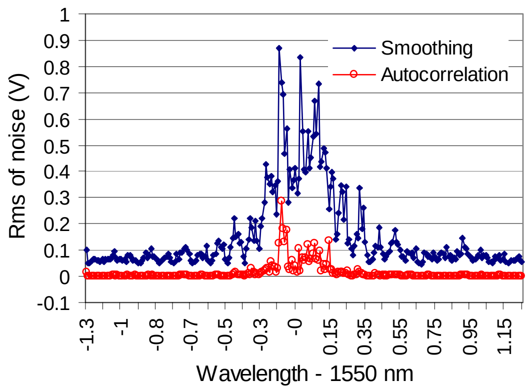


Fig.7 Noise effective values after signal processing as function of wavelength

Fig. 7 shows the noise effective values as function of the wavelength. In comparison with the original noise effective values (Fig. 3), the noise effective values are reduced by the both signal processing methods. Table 1 shows the noise reduction ratio.

Table 1 Noise reduction ratio $k_r$ of detectable strain when using digital signal processing ($k_r$=$\varepsilon_o$/$\varepsilon$, $\varepsilon_o$: original strain calculated with sampling data, $\varepsilon$: strain calculated with processed data)

| Method / Wavelength | Numeric Smoothing (NS) | Autocorrelation Function (ACF) | NS and ACF |
|---|---|---|---|
| 1549.86 nm | 1.17 | 6.30 | 8.61 |
| 1550.05 nm | 1.25 | 4.75 | 5.56 |

The strain sensitivity can reasonably be improved by using signal processing algorithms. With these algorithms, strain variations in the order of $10^{-10}$ can be detected.

## 4. EXAMPLES

The Bragg grating measuring system is tested in laboratory and field experiments. A Bragg grating is embedded in an experimental rock of 1.5 m length. A seismic signal with a frequency about 1.67 kHz is generated if a metallic ball excitation is applied on an end of rock in the axial direction. The measuring system records the seismic signal. Fig. 8 shows the original sampling signal and its autocorrelation function. The signal to noise ratio is reasonably improved by using the autocorrelation function.

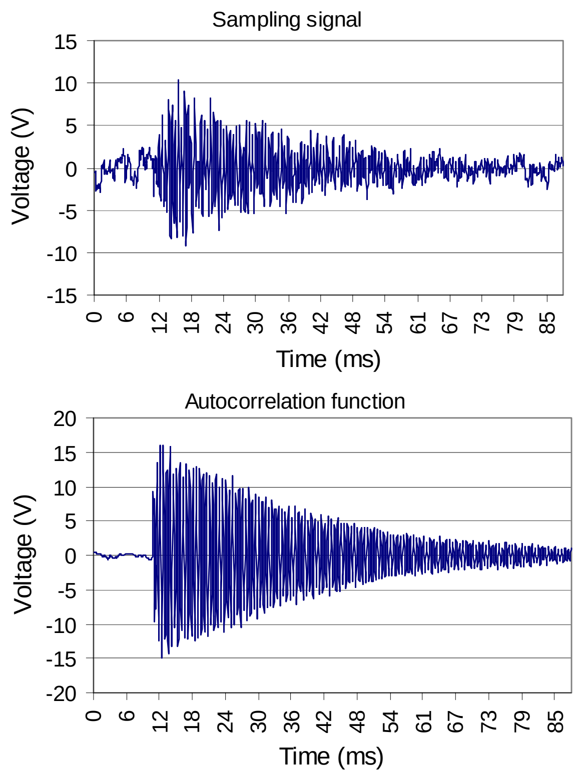


Fig. 8 Seismic signal generated with a metallic ball excitation in an experimental rock

The magnitude spectrum of the signals is shown in Fig. 9. The frequency component of the seismic signal is obviously amplified by using the autocorrelation function, while the noise frequency components are reduced.

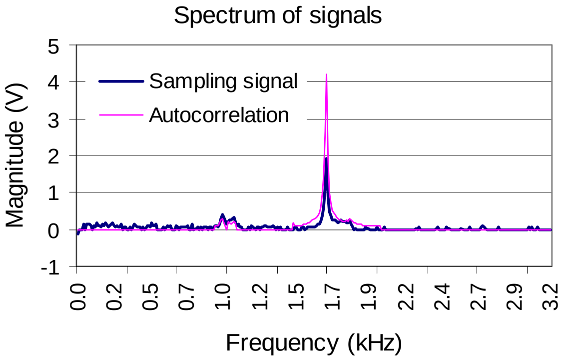


Fig. 9 Magnitude spectrum of sampling signal and autocorrelation function (laboratory measurements )

For field experiment an anchor with a Bragg grating is embedded in underground rock mass (Fig. 1). A seismic signal is generated with a hammer excitation in a distance of about 10 m from the embedded Bragg grating. Fig. 10 shows the detected signal and its autocorrelation function. The noise is effectively filtered with the autocorrelation function. The spectrum of the both signals is given in Fig. 11.

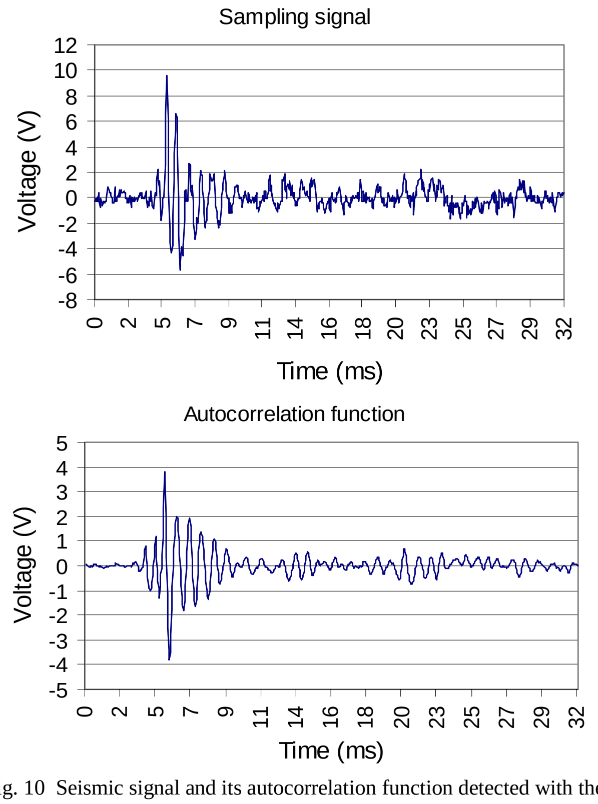


Fig. 10 Seismic signal and its autocorrelation function detected with the Bragg grating system in underground rock mass

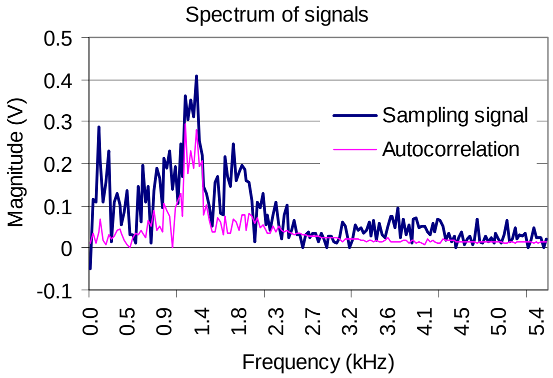


Fig. 11 Magnitude spectrum of sampling signal and autocorrelation function (field measurements)

## 4. CONCLUSIONS

For the measurement of dynamic seismic signals using a Bragg grating system the wavelength of the DFB-Laser is automatically optimized by measuring the dc photovoltage before the measurement. The noise influence caused by the instability of laser wavelength is reduced by the iterative smoothing and discrete autocorrelation function. Results from laboratory and field measurements show that the noise reduction of the autocorrelation method is very effective.
To further improve the sensitivity and the signal to noise ratio, the sensor structure must be optimized, and an optic band-pass filter, e.g. a Bragg grating controlled with peltier element or piezoceramic, should be integrated between the circulator and photodetector in the measuring system. These will be addressed in an further contribution.

## REFERENCES

[1] C. Schmidt-Hattenberger, G. Borm. and F. Amberg, Bragg grating seismic monitoring system, Proc. Photonics East 1999, Fiber Optic Sensor Technology and Applications, SPIE, Vol. 3860, pp. 417-424
[2] A. D. Kersey, et al, Fiber Bragg Grating Sensors, IEEE Journal of Lightwave Technology, vol. 15, pp.1442-1463, 1997
[3] C. Schmidt-Hattenberger, J.-G. Liu, G. Borm, Fiber Bragg Grating Seismic Monitoring System, 10. International Sensor-fairs and Conference, May 8-10, 2001, Nuremberg, Germany, vol. II, pp.303-307
[4] W. L. Schulz, J. P. Conte, E. Udd, and J. M. Seim, Static and dynamic testing of bridges and highways using long-gage fiber Bragg grating based strain sensors, Proc. Of SPIE vol. 4202, 2000, Industrial Sensing Systems, pp. 79-86
[5] E. Schrüfer, Signalverarbeitung - Numerische Verarbeitung digitaler Signale, 2. Auflage, Carl Hanser Verlag, München, Wien, 1992
[6] J.-G. Liu, Eigenkalibrierende Messverfahren und deren Anwendungen bei den Messungen elektrischer Größen, Fortschritt-Berichte VDI, Reihe 8: Mess-, Steuerungs- und Regelungstechnik, Nr. 830, VDI Verlag, Düsseldorf, 2000